Med Chem Res
DOI 10.1007/s00044-017-1829-6

MEDICINAL CHEMISTRY RESEARCH

ORIGINAL RESEARCH

Synthesis, computational studies and biological evaluation of new 1-acetyl-3-aryl thiourea derivatives as potent cholinesterase inhibitors

Aamer Saeed[1] · Muhammad Shakil Shah[2,3] · Fayaz Ali Larik[1] · Shafi Ullah Khan[2] · Pervaiz Ali Channar[1] · Ulrich Flörke[4] · Jamshed Iqbal[2]

Received: 18 September 2016 / Accepted: 1 March 2017

Abstract A new series of 1-acetyl-3-aryl thioureas **(3f1–15)** was synthesized by the reaction of acetyl isothiocyanate with a variety of suitably substituted aromatic anilines. The acetyl isothiocyanate was freshly prepared by reaction of corresonding acid chloride with potassium thiocyanate. The structural confirmation of all compounds was carried out by spectroscopic techniques and in case of **3a** by X-ray diffraction study. The newly prepared compounds were subjected to computational studies and evaluated for their cholinesterase (acetylcholinesterase and butyrylcholinesterase) inhibition studies. Except **3f9** and **3f15**, all the derivatives were found as selective inhibitor of acetylcholinesterase. Compound **3f2** ($IC_{50} \pm SEM = 1.99 \pm 0.11\ \mu M$) was found to be the most potent inhibitor of acetylcholinesterase exhibited ≈11 times greater inhibitory potential than reference inhibitor i.e. neostigmine ($IC_{50} \pm SEM = 22.2 \pm 3.2\ \mu M$). Compound **3f9** was found to be most potent butyrylcholinesterase inhibitor ($IC_{50} \pm SEM = 1.33 \pm 0.11\ \mu M$), exhibiting ≈four times greater selectivity for butyrylcholinesterase over acetylcholinesterase. Molecular docking studies were carried out to determine the binding site interactions of these potent inhibitors with cholinesterases and also supported the experimental observations.

Keywords Cholinesterases · Molecular docking · Potassium thiocynate · Substituted aniline

Introduction

Thioureas are well known organic compounds having thiocarbonyl group in their basic ring (Schroeder 1955; Mertschenk et al. 2002). Moreover, thioureas serve as valuable synthon in organic chemistry (Larik et al. 2016). The presence of oxygen and sulfur atoms in thiourea provides a site for metals to coordinate and form complexes (Koch 2001; Aly et al. 2007; Saeed et al. 2014). Different derivatives of thiourea have been used as basic precursor for the synthesis of various heterocyclic compounds and showed a diverse range of biological importance (Saeed et al. 2009). Among different classes of thiourea derivatives, acyl thioureas have gained considerable interest in the field of medicinal chemistry due to their numerous biological applications (Nencki 1873). Acyl thioureas exhibit a broad spectrum of bioactivities including antibacterial (Saeed et al. 2010), antifungal (Eweis et al. 2006), antitubercular (Sriram et al. 2007), herbicidal (Ke and Xue 2006), insecticidal (Brouwer and Grosscurt 1982,) as well

Electronic supplementary material The online version of this article (doi:10.1007/s00044-017-1829-6) contains supplementary material, which is available to authorized users.

✉ Aamer Saeed
aamersaeed@yahoo.com

✉ Jamshed Iqbal
drjamshed@ciit.net.pk

[1] Department of Chemistry, Quaid-I-Azam University, 45320 Islamabad, Pakistan

[2] Centre for Advanced Drug Research, COMSATS Institute of Information Technology, Abbottabad 22060, Pakistan

[3] Division of Analytical Chemistry, Institute of Chemical Science, Bahauddin Zakariya University, 60800 Multan, Pakistan

[4] Department Chemie, Fakultätfür Naturwissenschaften, Universität Paderborn, Warburgerstrasse 100, 33098 Paderborn, Germany

Published online: 30 March 2017

as corrosion resistant, antioxidants, and basic component in polymeric derivatives (Gopi et al. 2000). In addition to aroylthioureas, acylthiourea derivatives are also well known for their biological activities like bactericidal, fungicidal, herbicidal, insecticidal and as regulator of plant growth (Ren et al. 2000). However, thiourea may cause liver toxicity when coupled to the pharmaceutical drugs. It was shown in liver microsomes, in mammalian cells in culture (Ziegler 1978; Ziegler-Skylakakis 1998), and in intact rat liver (Krieter et al. 1984) that thiourea can form *S*-oxygenated products such as the reactive electrophiles formamidine sulfenic acid and formamidine sulfinic acid. The latter has been shown to be genotoxic in cultured mammalian cells (Ziegler-Skylakakis 1998).

Acetylcholinesterase (AChE, EC 3.1.1.7) and butyrylcholinesterase (BChE, EC 3.1.1.8) are serine-hydrolase enzymes that belong to a super family of estrases. Both isozymes have substantial similarities in their structures but show different specificities toward substrate and inhibitors due to the differences in amino acid sequences of their active sites (Marrs and Maynard 2013). These enzymes are present in different conducting tissues, however they are more active in motor neurons than in sensory neurons (Dave et al. 2000). BChE has higher activity in kidney, heart, intestine, liver, and lungs while AChE is more abundant in muscles, brain and erythrocyte membrane (Tougu 2001). The main function of these isozymes (AChE and BChE) is to catalyze the breakdown of neurotransmitter acetylcholine into choline and acetic acid (Koelle 1994) and thus terminate nerve impulse at cholinergic synapses (Shen et al. 2009). Normally, AChE degrades acetylcholine (ACh) to maximum extant and is responsible for the termination of signaling action (Terry and Buccafusco 2003). Moreover, it has been observed that AChE and BChE are found extensively higher in Alzheimer disease (AD). In the view of cholinergic hypothesis, Alzheimer's disease results from a lack of cholinergic function in the brain (Darvesh et al. 2003). A promising therapeutic strategy should be adopted for stimulating the central cholinergic functions. Recently, it has been reported that BChE act as therapeutic target site for ameliorating cholinergic dysfunction associated with AD, thus resulting in the regulation of synaptic ACh levels (Hardy and Selkoe 2002; Smith 2009).

Herein, we reported the synthesis of new series of 1-acetyl-3-aryl thiourea with complete characterization (FTIR, multinuclear NMR, single crystal XRD) along with their inhibitory potential against both AChE and BChE. Furthermore, docking studies were also carried out to predict the most plausible binding site interactions of potent inhibitors.

Results and discussion

Chemistry

*General procedure for the synthesis of 1-acetyl-3-aryl thioureas (**3f1–15**)*

A new series of thiourea derivatives **(3f1–15)** was synthesized by forming isothiocyanate intermediate. This intermediate was formed by the addition of acid chloride to the solution of potassium thiocyanide in the presence of dry acetone. The reaction was allowed to stand for 30 min. After 30 min, acetyl chloride was added to the potassium thiocyanide solution. Then the reaction mixture was allowed to cool and different aromatic substituted amines were incorporated as given in Scheme 1.

The characterization of all the synthesized aromatic substituted acyl thioureas was done on the basis of their spectroscopic data. ^{1}H and ^{13}C NMR spectra were recorded in deuterated DMSO-d_6 solvent. In ^{1}H NMR; two N–H protons at 11.87 and 11.34 ppm were appeared as singlets. These are the most deshielded signals because of intra molecular hydrogen bonding that result in shifting the signals towards higher ppm value, thus justify the presence of thio core in thiourea. The signal at 7–8 ppm region was clearly indicating the aromatic ring. The methyl of acyl group appeared at 2.35 ppm. The N–H proton lying in between thiocarbonyl and carbonyl is most deshielded due to intramolecular hydrogen bonding. The protons attached with benzene ring appeared in the usual range. In ^{13}C NMR, thiocarbonyl carbon appeared most deshielded at about 180 ppm and carbonyl carbon appeared at around 172–175 ppm. The vibrational analysis of synthesized compounds was investigated through IR spectroscopy. The characteristic broad peak of N–H bond appeared at 3200 cm^{-1}. The C–H sp^2 stretching frequency appeared at around 3000 cm^{-1}. The intense peak at around 1700–1600 cm^{-1} confirmed the presence of carbonyl group. The thiocarbonyl bond vibration appeared between 1050 and 1250 cm^{-1}.

In vitro cholinesterase inhibition studies and structure–activity relationship (SAR)

The inhibition studies of these synthesized compounds against AChE and BChE revealed that all compounds, except compound **3f9** and **3f15**, exhibited selective inhibition of AChE (Table 1). The compound 1-acetyl-3-(2,4-dimethylphenyl) thiourea (**3f2**) with $IC_{50} \pm SEM$ value 1.99 ± 0.11 μM was found to be the most potent inhibitor of AChE. This compound exhibited up to 11-fold higher inhibitory potential as compared to the reference inhibitor i.e. Neostigmine ($IC_{50} \pm SEM = 22.2 \pm 3.2$ μM).

Scheme 1 Synthetic route to new 1-acetyl-3-arylthiourea (**3f1–3f13** and **3f14** and **3f15**)

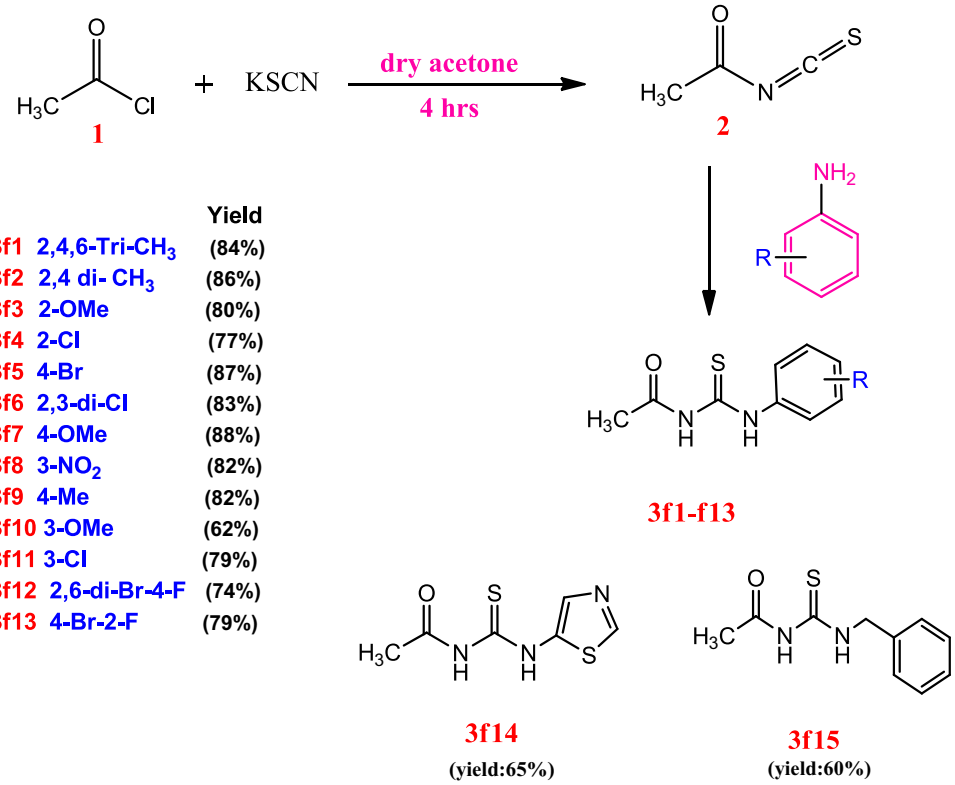

		Yield
3f1	2,4,6-Tri-CH_3	(84%)
3f2	2,4 di- CH_3	(86%)
3f3	2-OMe	(80%)
3f4	2-Cl	(77%)
3f5	4-Br	(87%)
3f6	2,3-di-Cl	(83%)
3f7	4-OMe	(88%)
3f8	3-NO_2	(82%)
3f9	4-Me	(82%)
3f10	3-OMe	(62%)
3f11	3-Cl	(79%)
3f12	2,6-di-Br-4-F	(74%)
3f13	4-Br-2-F	(79%)

Table 1 Acetylcholinesterase and butyrylcholinesterase inhibition studies in presence of the synthesized compounds

Code	AChE activity IC_{50} (μM) ± SEM	BChE activity
3f1	3.27 ± 0.44	<100
3f2	1.99 ± 0.11	<100
3f3	2.17 ± 0.56	<100
3f4	78.5 ± 3.56	<100
3f5	4.09 ± 0.26	<100
3f6	25.8 ± 2.52	<100
3f7	35.1 ± 3.11	<100
3f8	2.01 ± 0.11	<100
3f9	5.38 ± 0.62	1.33 ± 0.21
3f10	4.79 ± 0.63	<100
3f11	19.8 ± 1.04	<100
3f12	16.9 ± 0.98	<100
3f13	18.2 ± 1.03	<100
3f14	11.2 ± 1.32	<100
3f15	24.6 ± 2.09	3.02 ± 0.12
Neostigmine	22.2 ± 3.2	49.6 ± 6.11

The IC_{50} is the concentration at which 50% of the enzyme activity is inhibited. AChE and BChE activities were performed at the final concentration of 800 μM

From SAR based comparative analysis of compound **3f2** with the other derivatives, it was found that the inhibitory activity of 1-acetyl-3-(2,4-dimethylphenyl) thiourea (**3f2**) is more as compared to 1-acetyl-3-mesitylthiourea **(3f1)** having three methyl groups at ortho, para, and meta position. It can be inferred that the activity of compound (**3f2**) is due to the presence of the two methyl groups on benzene moiety i.e. one at ortho and other at para position that activate the ring by sigma pi conjugation. Other compounds exhibited inhibitory values in the range of IC_{50} ± SEM = 2.01 ± 0.11 to 78.5 ± 3.56 μM. Only two compounds i.e. 1-acetyl-3-(4-chlorophenyl) thiourea **(3f9)** and 1-acetyl 3-benzylthiourea **(3f15)** were found as potential inhibitors of BChE having the IC_{50} ± SEM value 1.33 ± 0.21 and 3.02 ± 0.12 μM, respectively. The compound **3f9** exhibited up to four times and compound **3f15** exhibited up to eight times greater selectivity for BChE over AChE inhibition. The reason for the maximum inhibition by these two compounds **3f9** and **3f15** might be due to presence of un-substituted benzene ring in compounds or substituted ring by less electronegative group i.e methyl group

Kinetics study

The potential inhibitors (**3f2** and **3f9**) with potent IC_{50} values were then selected for the kinetics study in order to determine their type of inhibition. Both compounds **3f2** and **3f9** exhibited non-competitive mode of inhibition against their respective AChE (Fig. 1) and BChE (Fig. 2) enzymes.

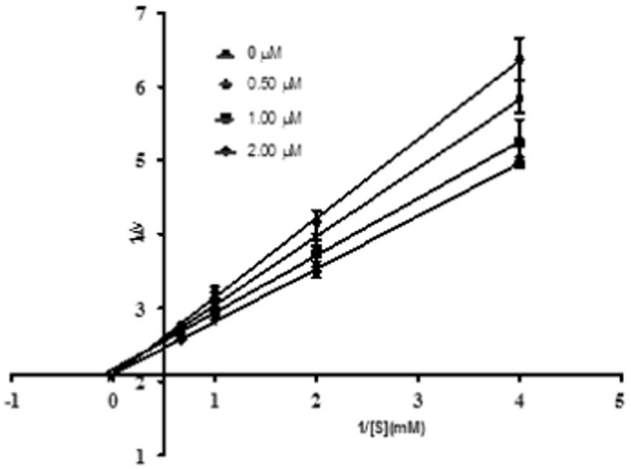

Fig. 1 Double-reciprocal plot of the inhibition kinetics of AChE by compound **3f2** indicating non-competitive inhibition. Changes in the initial velocities of the reaction were measured at different concentrations of the inhibitors using substrate acetylthiocholine chloride

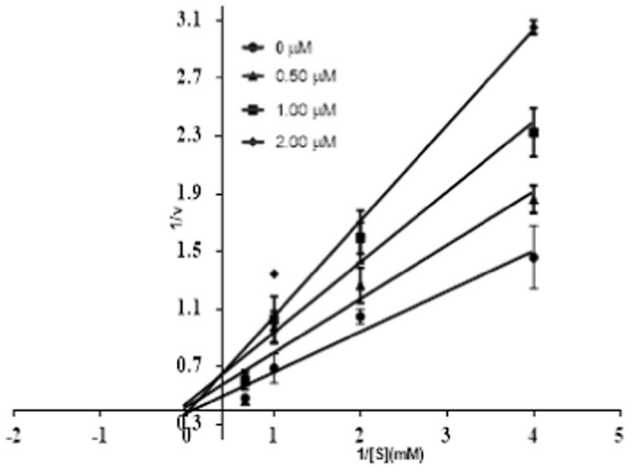

Fig. 2 Double-reciprocal plot of the inhibition kinetics of BChE by compound **3f9** indicating non-competitive inhibition. Changes in the initial velocities of the reaction were measured at different concentrations of the inhibitors using substrate butyrylthiocholine chloride

Molecular docking

Molecular docking studies against AChE and BChE

The putative binding mode of compound **3f2** (most potent inhibitor of AChE) was predicted inside the active site of AChE (Fig. 3). Analysing the key interactions of **3f2** within the active site of AChE revealed that compound **3f2** was entrenched by aromatic ring containing amino acids residue that is Trp86, Ala204, Phe297, Typ337, and Phe338 (Fig. 4). In its preferred docking pose, compound **3f2** is docked at the bottom of the active site gorge and almost coplanar with residues Trp86 and Tyr337. The central aromatic ring of the **3f2** is facing Trp86 and Tyr337 for making pi–pi stacked interaction. Ala204 and Gly121 make hydrogen bonding with the carbonyl group of **3f2**. In addition to this N6 also makes hydrogen bonding with the His447.

The plausible binding mode of **3f9** within the active site of BChE (Fig. 4) differs from the docked pose of compound **3f2** in the active site of AChE. The backbone of active site of BChE consists of Trp82, Gly116, Gly117, Ala199, Ser198, Glu197, and His438. The key interactions are in agreement with already reported bonding interactions such as aromatic stacking interaction to Trp82 and hydrogen bonding with the main chain carbonyl of His438. Critical analysis also revealed some other key hydrogen bonding interactions with Ser198 with Gly117 amino acid.

Conclusion

A new series of 1-acetyl-3-aryl thiourea derivatives was synthesized and characterized. When evaluated for their inhibitory potential against cholinesterases i.e. AChE and BChE, except compound **3f9** and **3f15** all the remaining derivatives were found to have selective inhibition of AChE over BChE activity. Compound **3f2** ($IC_{50} \pm SEM = 1.99 \pm 0.11$ µM) was found to be the most potent inhibitor of AChE. While, compound **3f9** was found to be most potent BChE inhibitor ($IC_{50} \pm SEM = 1.33 \pm 0.11$ µM), exhibiting ≈four times greater selectivity for BChE over AChE. It was also further validated from molecular docking studies that were carried out to determine the binding site interactions of potent inhibitors with cholinesterases.

Materials and methods

General

Melting points were recorded using a digital Gallenkamp (SANYO) model MPD.BM 3.5 apparatus. ^{1}H NMR spectra were determined in $CDCl_3$ and DMSO solutions at 300 MHz using a Bruker AM-300 spectrophotometer while TMS was used as an internal reference. Similarly, ^{13}C NMR spectra were determined at 75 MHz using a Bruker 75 MHz NMR spectrometer in $CDCl_3$ solution. FTIR spectra were recorded on an FTS 3000 MX spectrophotometer. Elemental analyses were conducted using a LECO-183 CHNS analyzer. The reactions were monitored by TLC using Pre-coated Silicagel-60 HF254 TLC plates.

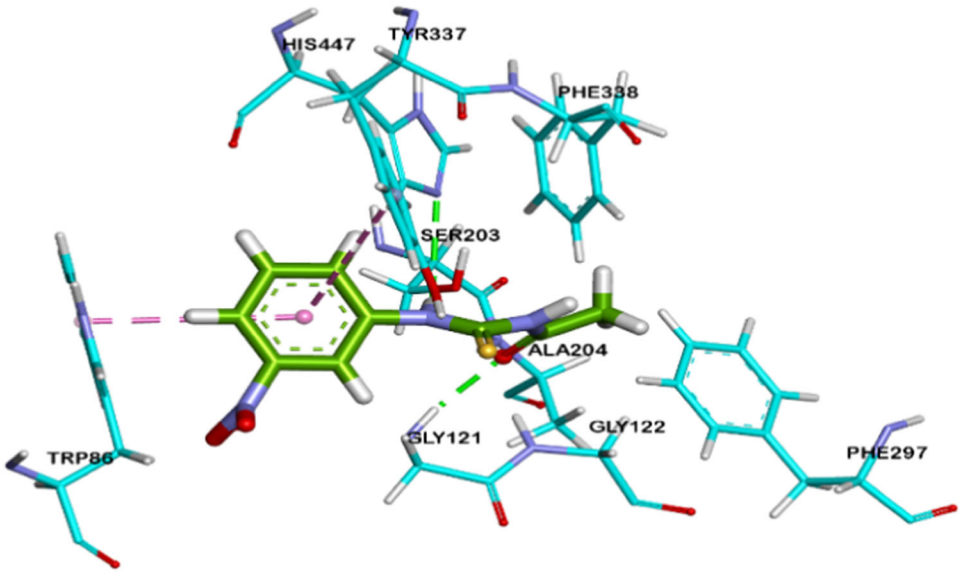

Fig. 3 Putative binding mode of **3f2** (most potent inhibitor AChE, *green colored*) in active site of AChE (*light cyan colored*) (color figure online)

Experimental data

*Synthesis of 1-acetyl-3-aryl thiourea (**3f1–3f15**)*

The required chemicals were purchased from sigma Aldrich and were dried and distilled according to standard procedures. The progress of reaction was monitored by thin layer chromatography (TLC). The synthesized derivatives were filtered and washed with *n*-hexane. The crude product obtained was dried and then recrystallized in ethanol solvent to get the pure product.

*1-Acetyl-3-mesitylthiourea (**3f1**)*

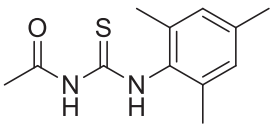

White crystalline solid, m.p = 199 °C, yield = 84%, R_f = 0.58 (*n*-Hexane:ethyl acetate 1:1) FTIR υ (cm^{-1}) 3188.3 (N–H, stretching), 2999.5 (Aromatic C–H, stretching), 1689.2 (C=O, stretching), 1578 (N–O, bending), 1507.5 (C–C, stretching), 1411.6 (C–H, bending), 1332.99 (N–O, bending), 1250.8 (C=S, stretching). ^{1}H NMR (DMSO-d6, 300 MHz,); δ (ppm) 11.66 (s, 1H, NH), 11.45 (s, 1H, NH), 6.90 (2H Ar–H), 2.51 (s, 3H), 2.24 (s, 6H Ar 2 × CH_3), 2.10 (s, 3H Ar–CH_3); ^{13}C NMR (75 MHz DMSO-d6) δ (ppm) 180 (C=S), 172.9(C=O), 136.9, 135.0, 133.8, 128.9 (Ar–C), 24.17, 21.0, 18.20 (CH_3), anal. calcd. for $C_{12}H_{16}N_2OS$: C, 60.99; H, 6.82; N, 11.85; S, 13.57 found: C, 60.97; H, 6.84; N, 11.84; S, 13.58.

*1-Acetyl-3-(2, 4-dimethylphenyl) thiourea (**3f2**)*

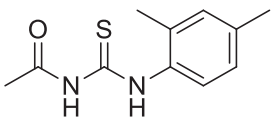

Light yellow solid, m.p = 190 °C, yield = 86%, R_f = 0.62 (n-Hexane:Ethyl acetate 1:1) FTIR υ (cm^{-1}) 3182.1 (N–H, stretching), 2997.5 (Aromatic C–H, stretching), 1683.2 (C=O, stretching), 1573 (N–O, bending), 1509.5 (C–C, stretching), 1413.2 (C–H, bending), 1335.95 (N–O, bending), 1255.3 (C=S, stretching). ^{1}H NMR (DMSO-d6, 300 MHz,); δ (ppm) 11.66 (s, 1H, NH), 11.45 (s, 1H, NH), 6.9–7.39 (m, 3H Ar–H), 2.49 (s, 3H), 2.21 (s, 6H Ar 2 × CH_3); ^{13}C NMR (75 MHz DMSO-d6) δ (ppm) 178 (C=S), 171.9 (C=O), 138.9, 134.1, 133.5, 132.5, 128.7, 126.5 (Ar–C), 21.0, 18.20 (CH_3), anal. calcd. for $C_{11}H_{14}N_2OS$: C, 59.43; H, 6.35; N, 12.60; S, 14.42 found: C, 59.41; H, 6.37; N, 12.63; S, 14.45.

*1-Acetyl-3-(2-methoxyphenyl) thiourea (**3f3**)*

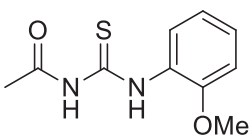

Brown crystalline solid, m.p = 190 °C, yield = 80%, R_f = 0.62 (n-Hexane:Ethyl acetate 1:1) FTIR υ (cm^{-1}) 3170.5 (N–H, stretching), 2915.5 (Aromatic C–H, stretching), 1670.5 (C=O, stretching), 1560 (N–O, bending), 1504.2 (C–C, stretching), 1419.2 (C–H, bending), 1310.61 (N–O, bending), 1292.8 (C=S, stretching). ^{1}H NMR (DMSO-d6,

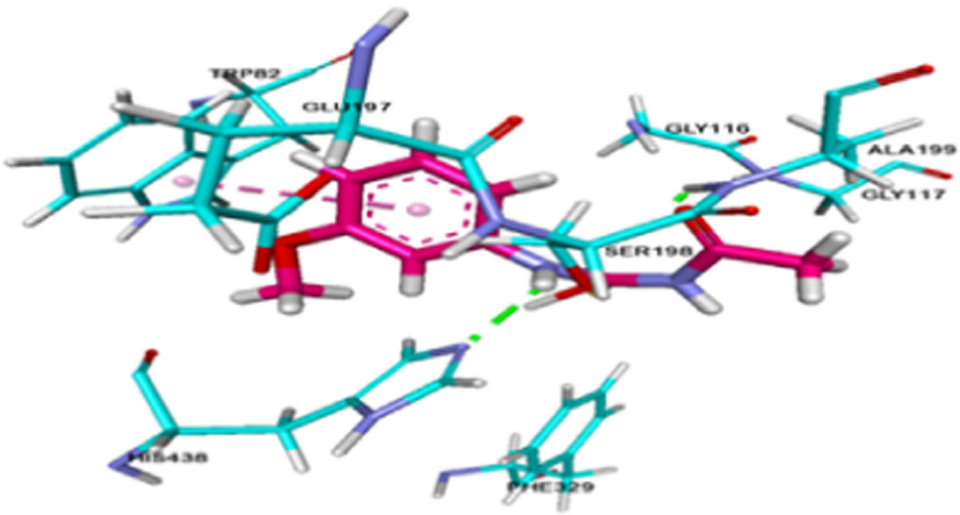

Fig. 4 Putative binding mode of **3f9** (most potent inhibitor BChE, *maroon colored*) in active site of BChE (*light cyan colored*) (color figure online)

300 MHz,); δ (ppm) 11.90 (s, 1H, NH), 11.70 (s, 1H, NH), 7.12 (d, 2H, $J = 7.8$ Hz ArH), 6.83(Ar–H, d, 2H, $J = 7.7$ Hz), 3.88 (s, 3H), 2.40 (s, 3H); ^{13}C NMR (75 MHz DMSO-d6) δ (ppm) 177 (C=S), 165.2 (C=O), 131.1, 130.1, 127.2, 124.8 (Ar–C), 23 (CH_3), 55 (CH_3), anal. calcd. for $C_{10}H_{12}N_2O_2S$: C, 53.58; H, 5.41; N, 12.51; S, 14.31 found: C, 53.43; H, 5.30; N, 12.32; S, 14.15.

*1-Acetyl-3-(2-chlorophenyl) thiourea (**3f4**)*

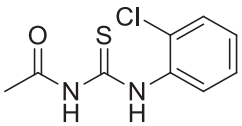

Light yellow solid, m.p = 188 °C, yield = 77%, R_f = 0.52 (n-Hexane:Ethyl acetate 1:1) FTIR υ (cm^{-1}) 3186.2 (N–H, stretching), 2994.3 (Aromatic C–H, stretching), 1687.2 (C=O, stretching), 1571 (N–O, bending), 1507.1 (C–C, stretching), 1415.3 (C–H, bending), 1337.91 (N–O, bending), 1295.3 (C=S, stretching). ^{1}H NMR (DMSO-d6, 300 MHz,); δ (ppm) 11.77 (s, 1H, NH), 11.55 (s, 1H, NH), 7.73 (d, 2H, $J = 7.8$ Hz ArH), 7.47 (Ar–H, d, 2H, $J = 7.8$ Hz) 2.43 (s, 3H); ^{13}C NMR (75 MHz DMSO-d6) δ (ppm) 187 (C=S), 170.1 (C=O), 134.1, 132.5, 128.7, 126.5 (Ar–C), 23 (CH_3), anal. calcd. for $C_9H_9ClN_2OS$: C, 47.25; H, 3.98; N, 12.25; S, 14.02 found: C, 47.28; H, 3.95; N, 12.23; S, 14.06.

*1-Acetyl-3-(4-bromophenyl) thiourea (**3f5**)*

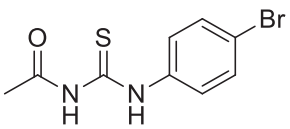

White crystalline solid, m.p = 186 °C, yield = 87%, R_f = 0.42 (n-Hexane:Ethyl acetate 1:1) FTIR υ (cm^{-1}) 3189.5 (N–H, stretching), 2995.5 (Aromatic C–H, stretching), 1685.5 (C=O, stretching), 1579 (N–O, bending), 1509.8 (C–C, stretching), 1419.5 (C–H, bending), 1338.93 (N–O, bending), 1296.5 (C=S, stretching). ^{1}H NMR (DMSO-d6, 300 MHz,); δ (ppm) 11.79 (s, 1H, NH), 11.65 (s, 1H, NH), 7.66 (d, 2H, $J = 7.7$ Hz ArH), 7.43(Ar–H, d, 2H, $J = 7.7$ Hz) 2.44 (s, 3H); ^{13}C NMR (75 MHz DMSO-d6) δ (ppm) 182 (C=S), 169.2 (C=O), 132.1, 131.1, 128.2, 125.8 (Ar–C), 20 (CH_3), anal. calcd. for $C_9H_9BrN_2OS$:C, 39.55; H, 3.38; N, 10.26; S, 11.71 found: C, 39.41; H, 3.28; N, 10.17; S, 11.65.

*1-Acetyl-3-(2, 3-dichlorophenyl) thiourea (**3f6**)*

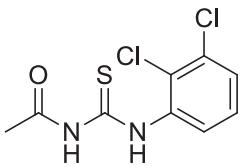

Light yellow solid, m.p = 178 °C, yield = 83%, R_f = 0.48 (n-Hexane:Ethyl acetate 1:1) FTIR υ (cm^{-1}) 3180.2 (N–H, stretching), 2984.3 (Aromatic C–H, stretching), 1687.2 (C=O, stretching), 1565 (N–O, bending), 1502.1 (C–C, stretching), 1411.3 (C–H, bending), 1331.91 (N–O, bending), 1290.3 (C=S, stretching). ^{1}H NMR (DMSO-d6, 300 MHz,); δ (ppm) 11.79 (s, 1H, NH), 11.65 (s, 1H, NH), 7.74 (d, 2H, $J = 7.9$ Hz ArH), 7.47(Ar–H, d, 2H, $J = 7.6$ Hz) 2.40 (s, 3H); ^{13}C NMR (75 MHz DMSO-d6) δ (ppm) 185 (C=S), 174.1 (C=O), 136.1, 133.5, 1297, 127.5 (Ar–C), 21 (CH_3), anal. calcd. for $C_9H_9Cl_2N_2OS$:C, 47.25; H, 3.98; N, 12.25; S, 14.02 found: C, 47.28; H, 3.95; N, 12.23; S, 14.06.

*1-Acetyl-3-(4-methoxyphenyl) thiourea (**3f7**)*

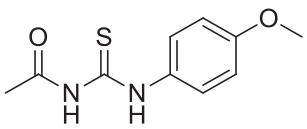

Brown crystalline solid, m.p = 180 °C, yield = 88%, R_f = 0.82 (n-Hexane:Ethyl acetate 1:1) FTIR υ (cm^{-1}) 3179.5 (N–H, stretching), 2985.5 (Aromatic C–H, stretching), 1675.5 (C=O, stretching), 1569 (N–O, bending), 1504.2 (C–C, stretching), 1416.2 (C–H, bending), 1337.61 (N–O, bending), 1292.8 (C=S, stretching). ^{1}H NMR (DMSO-d6, 300 MHz,); δ (ppm) 11.99 (s, 1H, NH), 11.77 (s, 1H, NH), 7.12 (d, 2H, J = 7.6 Hz ArH), 6.83(Ar–H, d, 2H, J = 7.6 Hz), 3.88 (s, 3H), 2.40 (s, 3H);^{13}C NMR (75 MHz DMSO-d6) δ (ppm) 181 (C=S), 169.2 (C=O), 131.1, 130.1, 127.2, 124.8 (Ar–C), 19 (CH_3), 59(CH_3), anal. calcd. for $C_{10}H_{12}N_2O_2S$: C, 53.58; H, 5.41; N, 12.51; S, 14.31 found: C, 53.43; H, 5.30; N, 12.45; S, 14.22.

*1-Acetyl-3-(3-nitrophenyl) thiourea (**3f8**)*

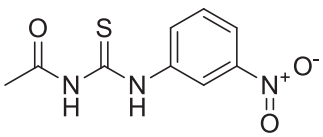

Yellow crystalline solid, m.p = 215 °C, yield = 82%, R_f = 0.61 (n-Hexane:Ethyl acetate 1:1) FTIR υ (cm^{-1}) 3199.1 (N–H, stretching), 2984.1 (Aromatic C–H, stretching), 1685.8 (C=O, stretching), 1589 (N–O, bending), 1509.8 (C–C, stretching), 1419.7 (C–H, bending), 1337.87 (N–O, bending), 1299.2 (C=S, stretching). ^{1}H NMR (DMSO-d6, 300 MHz,); δ (ppm) 12.80 (s, 1H, NH), 11.88 (s, 1H, NH), 7.89–7.32 (m, 4H, ArH), 2.33 (s, 3H); ^{13}C NMR (75 MHz DMSO-d6) δ (ppm) 189.1 (C=S), 170.5 (C=O), 146.4, 139.2, 136.7, 132.2, 129.2, 127.6 (Ar–C), 20 (CH_3), anal. calcd. for $C_9H_9N_3O_3S$: C, 45.17; H, 3.76; N, 17.59; S, 13.41 found: C, 46.19; H, 4.77; N, 18.58; S, 14.43.

*1-Acetyl-3-(4-methylphenyl) thiourea (**3f9**)*

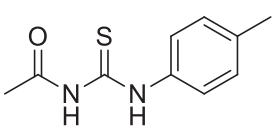

Light yellow solid, m.p = 188.2 °C, yield = 82%, R_f = 0.64 (n-Hexane:Ethyl acetate 1:1) FTIR υ (cm^{-1}) 3178.8 (N–H, stretching), 2989.5 (Aromatic C–H, stretching), 1688.2 (C=O, stretching), 1595 (N–O, bending), 1515.5 (C–C, stretching), 1421.5 (C–H, bending), 1341.57 (N–O, bending), 1291.3 (C=S, stretching). ^{1}H NMR (DMSO-d6, 300 MHz); δ (ppm) 12.53 (s, 1H, NH), 11.92 (s, 1H, NH), 7.26–6.8 (ArH, m, 4H), 2.29 (s, 3H); 2.11 (s, 3H); ^{13}C NMR (75 MHz DMSO-d6) δ (ppm) 183.7 (C=S), 168.9 (C=O), 137.4, 134.2, 131.7, 129.2, 128.2, 126.4 (Ar–C), 25, 20 (CH_3), –. for $C_{10}H_{12}N_2OS$: C, 47.29; H, 3.95; N, 12.24; S, 14.01 found: C, 47.13; H, 3.77; N, 12.16; S, 14.95.

*1-Acetyl-3-(3-methoxyphenyl) thiourea (**3f10**)*

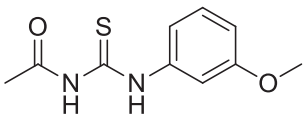

Red solid, m.p = 212 °C, yield = 62%, R_f = 0.57 (n-Hexane:Ethyl acetate 1:1) FTIR υ (cm^{-1}) 3188.2 (N–H, stretching), 2985.7 (Aromatic C–H, stretching), 1687.4 (C=O, stretching), 1590 (N–O, bending), 1510.5 (C–C, stretching), 1420.5 (C–H, bending), 1339.57 (N–O, bending), 1289.3 (C=S, stretching). ^{1}H NMR (DMSO-d6, 300 MHz,); δ (ppm) 12.11 (s, 1H, NH), 11.82 (s, 1H, NH), 7.35–6.9 (ArH, m, 4H), 3.89 (CH_3), 2.33 (s, 3H); ^{13}C NMR (75 MHz DMSO-d6) δ (ppm) 185.1 (C=S), 175.5 (C=O), 136.4, 133.2, 130.7, 128.2, 127.2, 125.6 (Ar–C), 55 (CH_3), 20 (CH_3), anal. calcd. for $C_{10}H_{12}N_2O_2S$: C, 53.57; H, 5.37; N, 12.49; S, 14.31 found: C, 53.49; H, 5.24; N, 12.38; S, 14.15.

*1-Acetyl-3-(3-chlorophenyl) thiourea (**3f11**)*

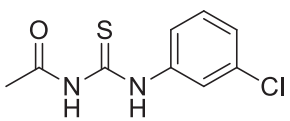

White crystalline solid, m.p = 199.5 °C, yield = 79%, R_f = 0.71 (n-Hexane:Ethyl acetate 1:1) FTIR υ (cm^{-1}) 3185.2 (N–H, stretching), 2998.3 (Aromatic C–H, stretching), 1691.2 (C=O, stretching), 1581 (N–O, bending), 1507.7 (C–C, stretching), 1415.8 (C–H, bending), 1337.51 (N–-O, bending), 1297.2 (C=S, stretching). ^{1}H NMR (DMSO–d6, 300 MHz,); δ (ppm) 11.78 (s, 1H, NH), 11.59 (s, 1H, NH), 7.75–6.92 (Ar–-H, m, 4H), 2.36 (s, 3H); ^{13}C NMR (75 MHz DMSO-d6) δ (ppm) 183 (C=S), 173.5 (C=O), 137.1, 135.5, 129.7, 128.2, 126.2 (Ar–C), 23 (CH_3), anal. calcd. for $C_{10}H_{10}ClNOS$: C, 52.71; H, 4.45; N, 6.17; S, 14.04 found: C, 52.63; H, 4.29; N, 5.97; S, 13.98.

*1-Acetyl-3-(2, 6-dibromo-4-fluorophenyl) thiourea (**3f12**)*

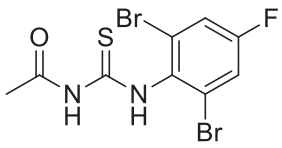

Brown solid, m.p = 209 °C, yield = 74%, $R_f = 0.55$ (n-Hexane:Ethyl acetate 1:1) FTIR υ (cm−1) 3189.5 (N–H, stretching), 2991.8 (Aromatic C–H, stretching), 1689.8 (C=O, stretching), 1580 (N–O, bending), 1509.3 (C–C, stretching), 1414.3 (C–H, bending), 1382.19 (N–O, bending), 1257.8 (C=S, stretching). ^{1}H NMR (DMSO-d6, 300 MHz,); δ (ppm) 11.76 (s, 1H, NH), 11.55 (s, 1H, NH), 7.50 (Ar–H,2H), 2.51 (s, 3H); ^{13}C NMR (75 MHz DMSO-d6) δ (ppm) 185 (C=S), 178.9 (C=O), 139.9, 136.0, 134.8, 130.9 (Ar–C), 20 (CH_3), anal. calcd. for $C_9H_7Br_2FN_2OS$:C, 29.24; H, 1.92; N, 7.57; S, 8.67 found: C, 29.17; H, 1.83; N, 7.44; S, 8.56.

*1-Acetyl-3-(4-bromo-2-fluorophenyl) thiourea (**3f13**)*

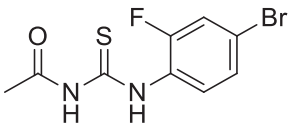

Yellow crystalline solid, m.p = 205 °C, yield = 79%, R_f = 0.68 (n-Hexane:Ethyl acetate 1:1) FTIR υ (cm^{-1}) 3185.3 (N–H, stretching), 2996.4 (Aromatic C–H, stretching), 1685.3 (C=O, stretching), 1575 (N–O, bending), 1509.7 (C–C, stretching), 1417.3 (C–H, bending), 1345.97 (N–O, bending), 1259.3 (C=S, stretching). ^{1}H NMR (DMSO-d6, 300 MHz,); δ (ppm) 11.61 (s, 1H, NH), 11.41 (s, 1H, NH), 7.35–6.9 (Ar–H, m, 3H), 2.45 (s, 3H); ^{13}C NMR (75 MHz DMSO-d6) δ (ppm) 182 (C=S), 175.6 (C=O), 140.9, 137.1, 135.1, 131.5, 127.7, 125.5 (Ar–C), 23 (CH_3), anal. calcd. for $C_9H_8BrFN_2OS$:C, 37.15; H, 2.77; 6.55; N, 9.62S, 11.04 found: C, 37.99; H, 2.68; N, 9.51S, 10.95.

*1-Acetyl-3-(thiazol-5-yl) thiourea (**3f14**)*

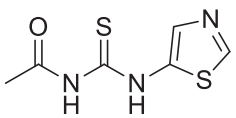

Reddish brown solid, m.p = 218 °C, yield = 65%, R_f = 0.71 (n-Hexane:Ethyl acetate 1:1) FTIR υ (cm^{-1}) 3189.8 (N–H, stretching), 2989.7 (Aromatic C–H, stretching), 1686.5 (C=O, stretching), 1591 (N–O, bending), 1511.8 (C–C, stretching), 1421.5 (C–H, bending), 1345.57 (N–O, bending), 1289.3 (C=S, stretching). ^{1}H NMR (DMSO-d6, 300 MHz,); δ (ppm) 11.80 (s, 1H, NH), 11.43 (s, 1H, NH), 7.69–7.26 (d, 2H, ArH), 2.27 (s, 3H); ^{13}C NMR (75 MHz DMSO-d6) δ (ppm) 185.2 (C=S), 174.5 (C=O), 153.4, 146.2, 136.7, 127.6 (Ar–C), 22 (CH_3), anal. calcd. for $C_6H_7N_3OS_2$: C, 35.83; H, 3.53; N, 20.87; S, 31.83 found: C, 35.75; H, 3.45; N, 20.70; S, 31.73.

*1-Acetyl-3-benzylthiourea (**3f15**)*

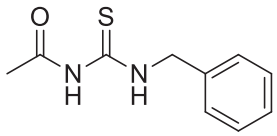

Red solid, m.p = 179 °C, yield = 60%, R_f = 0.51 (n-Hexane:Ethyl acetate 1:1) FTIR υ (cm^{-1}) 3169.8 (N–H, stretching), 2949.7 (Aromatic C–H, stretching), 1676.5 (C=O, stretching), 1581 (N–O, bending), 1515.8 (C–C, stretching), 1431.5 (C–H, bending), 1355.37 (N–O, bending), 1289.7 (C=S, stretching). ^{1}H NMR (DMSO-d6, 300 MHz,); δ (ppm) 11.87 (s, 1H, NH), 11.53 (s, 1H, NH), 7.26–6.9 (ArH, dd, 3H), 3.95 (s, 2H), 2.27 (s, 3H); ^{13}C NMR (75 MHz DMSO-d6) δ (ppm) 188.7 (C=S), 173.5 (C=O), 143.4, 129.2, 127.6 (Ar–C), 47 (CH_2), 22 (CH_3), anal. calcd. for $C_{10}H_{12}N_2OS$: C, 57.65; H, 5.82; N, 13.47; S, 15.41 found: C, 58.69; H, 6.83; N, 14.49; S, 15.45

Structure determinationof 3f1

$C_{12}H_{16}N_2OS$, $M_r = 236.3$, colourless crystal, size 0.47 × 0.21 × 0.18 mm^3, triclinic space group ***P -1*** with $Z = 4$, a = 8.2324, $b = 11.2356$, $c = 13.7870$ Å, $\alpha = 89.981(2)°$, β = 84.542(2)°, $\gamma = 85.393(2)°$, $V = 1265.3$ (2) Å^3; $D_c = 1.241$ Mg/m^3, $\mu = 0.238$ mm^{-1}, $F(000) = 504$. The intensity data was recorded using a Bruker SMART CCD area-detector diffractometer with graphite monochromated MoK$_\alpha$ radiation ($\lambda = 0.71073$ Å) at $T = 130(2)$ K. 7562 reflections collected $1.5 > \Theta > 27.9°$; 5595 independent reflections $I > 2\sigma$ (I), $R_{int} = 0.010$. Structure solution was carried out by direct method (Sheldrick 2008) and full-matrix least squares refinement was done based on F^2 and 297 parameters. Hydrogen atoms were refined anisotropically and were clearly located from difference Fourier maps Moreover they were also refined at idealized positions riding on the carbon atoms with isotropic displacement parameters $U_{iso}(H) = 1.2U_{eq}$(C/N) or $1.5U_{eq}$(CH_3) and C–H 0.98–1.00 and N–H 0.88 Å. There are two crystallographically independent but chemically equal molecules A and B per asymmetric unit. Refinement converged at $R1 = 0.039$ [$I > 2\sigma(I)$], w$R2 = 0.107$ [*all data*] and $S = 1.03$; min./max. ΔF -0.24/ 0.37 e/Å^3.

Crystallographic data (excluding structure factors) for the structure reported in this paper have been deposited with the Cambridge Crystallographic Data Centre as supplementary

publication no. CCDC-1437229. Copies of available material can be obtained free of charge via www.ccdc.cam.ac.uk/data_request/cif, by e-mailing data_request@ccdc.cam.ac.uk, or contacting the Cambridge Crystallographic Data Centre, 12, Union Road, Cambridge CB2 1EZ, UK; fax: + 44 1223 336033.

Computational study

The geometry of the synthesized compounds was optimized with DFT/B3LYP as implemented in Guassian-09 (Gaussian09 2009) quantum chemistry package. Using the DFT/B3LYP calculation method with 6–311++G(d,p) basis set in the ground state, the optimized molecular geometric parameters were performed. The energy gap between highest occupied molecular orbital (HOMO) and lowest unoccupied molecular orbital (LUMO) is a critical parameter to determine molecular electrical transport properties (Fukui 1982; Gökce and Bahçeli 2013). By analyzing HOMO and LUMO energy values, molecular properties, such as the chemical reactivity, kinetic stability, optical polarizability, chemical hardness and softness, and electronegativity can be accessed. HOMO–LUMO energies were calculated and are summarized in Table 2 while the shape of orbitals is shown in Fig. 5. The oxidation and reduction potential of **3f10** is observed to be least among the other thioureas and is in accordance with the computed HOMO and LUMO values (Table 2), which can be attributed to the presence of methoxy group at the meta position of phenyl ring. It can also be seen in Fig. 5 that the orbitals are polarized to a much greater extent in **3f15**, **3f14**, **3f4** in comparison to other thioureas, owing to the presence of a more polar methoxy group on the phenyl ring. The calculated values were found to be well in agreement with the experimental values calculated via cyclic voltametry.

Table 2 Observed oxidation and reduction potentials in cyclic voltametry and computed HOMO, LUMO values

Sample code	Oxidation potential (V)	HOMO (eV)	Reduction potential (V)	LUMO (eV)
3f1	−0.20621	−0.20938	−0.03583	−0.04381
3f2	−0.20695	−0.20893	−0.04322	−0.04561
3f3	−0.22519	−0.22429	−0.07404	−0.07301
3f4	−0.2236	−0.22225	−0.07361	−0.07250
3f5	−0.21438	−0.21329	−0.04746	−0.04835
3f7	−0.22135	−0.21126	−0.06241	−0.05342
3f8	−0.02391	−0.22928	−0.12118	−0.11107
3f10	−033457	−0.31348	−0.24852	−0.24943
3f12	−0.2246	−0.21561	−0.05457	−0.05647
3f14	−0.24740	−0.23830	−0.15385	−0.14294
3f15	−0.31563	−0.21572	−0.04717	−0.05818

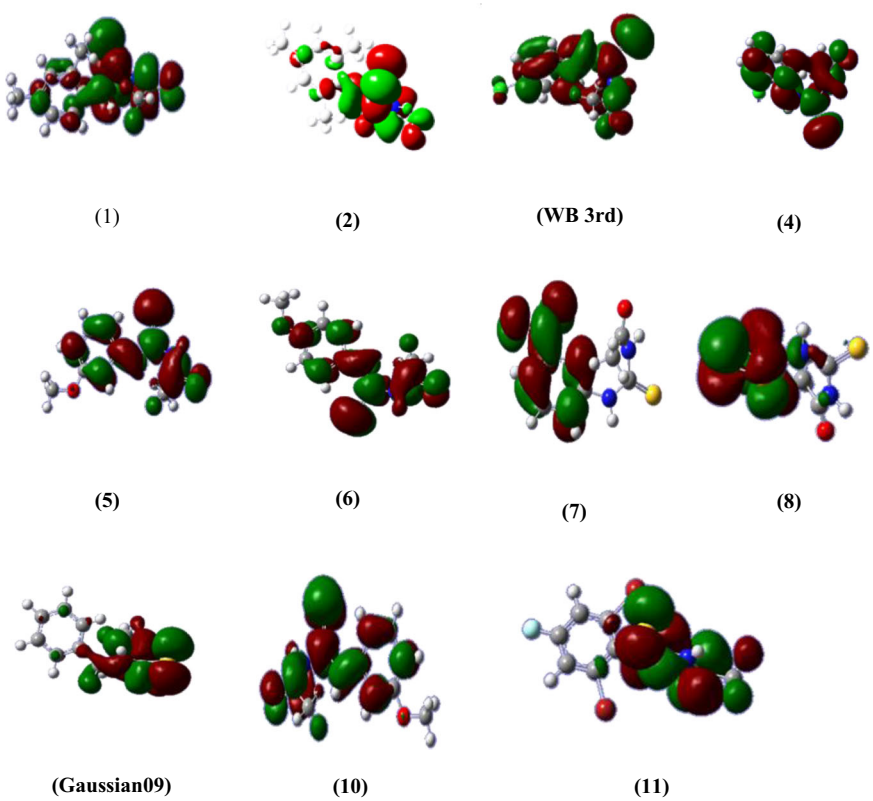

Fig. 5 Orbital diagrams of compound **3f1–14**, where **1** = 3f1, **2** = 3f2, **WB 3rd** = 3f3, **4** = 4f4, **5** = 3f5, **6** = 3f7, **7** = 3f8, **8** = 3f14, **Gaussian09** = 3f15, **10** = 3f10, **11** = 3f12

Structure discussion

The asymmetric unit contains two crystallographically independent but chemically equal molecules A and B with numbering schemes X1nn for A and X2nn for B (Fig. 6). Geometric parameters for both A and B exhibit no unexpected features, bond lengths and angles for both are equal, but the thiourea moiety of B is somewhat more twisted than that of A as may be seen from the torsion angles N22-C201-N21-C202 −8.9(2)°, C201-N21-C202-O2 8.8(2)° for B and N12-C101-N11-C102 0.6(2)°, C101-N11-C102-O1 −2.9 (2)° for A. The thiourea conformations are connected with intramolecular N12-H…O1 and N22-H…O2 bonds that form S(6) rings. The thiourea planes are almost perpendicular to the aromatic ring planes with torsion angles C101-N12-C104-C105 103.4(2)° and C201-N22-C204-C205 104.7(2)°, respectively.

In the crystal packing (Fig. 7) N–H…S interactions connect molecules with (N11)H..S1^{i} *(-x + 1, -y + 2, -z)* 2.54Å, N11-H..S1^{i} 160.8° and (N21)H…S2^{ii} *(-x + 1, -y, -z + 1)* 2.53Å, N2-H…S2^{ii} 165.3° into centrosymmetricAA^{i} and BB^{ii} dimers that are stacked along the *b*-axis

Biochemical assays

Acetylcholinesterase and butyrylcholinesterase inhibition assay

AChE and BChE inhibitory studies of synthesized derivatives were measured by using the reported Ellman's method with slight modifications (Ellman et al. 1961). Briefly, total reaction volume was kept as 100 µL, containing 60 µL of phosphate buffer (50 mM KH_2PO_4 pH 7.7), 10 µL of test compound (800 µM per well), followed by the addition of

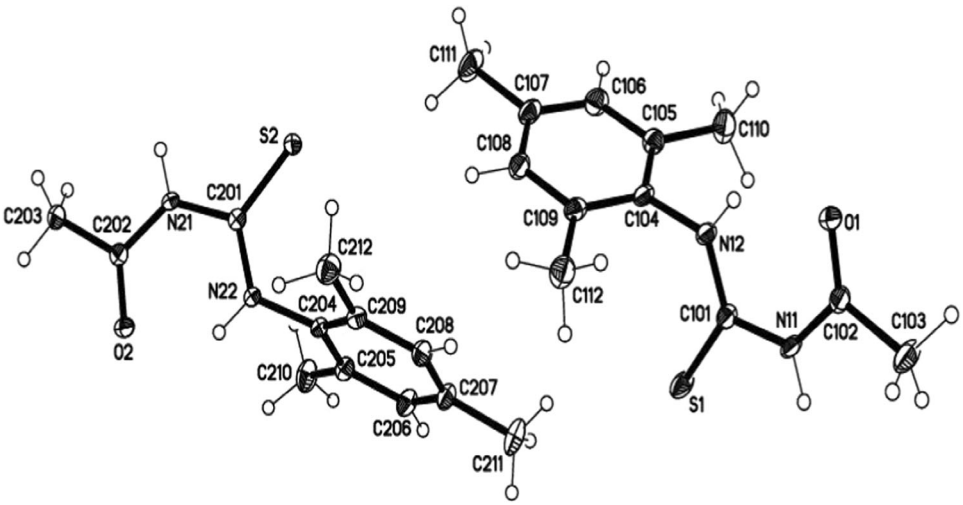

Fig. 6 Molecular structure of **3f1** showing both independent molecules A (1nn) and B (2nn). Anisotropic displacement ellipsoids are drawn at the 50% probability level

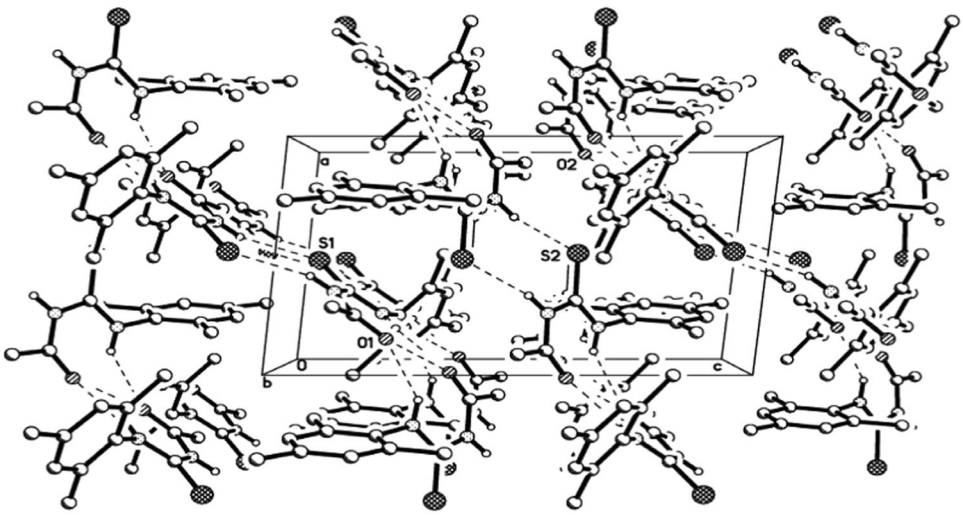

Fig. 7 Crystal packing of **3f1** viewed along [010] with intermolecular hydrogen bonds as dotted lines. H-atoms not involved are omitted

10 µL of AChE (0.015 unit per well) or 10 µL of BChE (0.1 unit per well). The contents of the well were mixed homogenously and incubated at 37 °C for 10 min and optical density was measured at 405 nm using 96-well plate reader (Bio-TekELx 800TM, Instruments, Inc.). The reaction was initiated by addition of 10 µL of acetylthiocholine chloride or butyrylthiocholine chloride as substrate (0.5 mM per well) followed by addition of 10 µL of coloring reagent DTNB (5, 5′- dithiobis-2- nitro benzoic acid). The reaction mixture was incubated at 37 °C for 20 min and optical density was measured at 405 nm. Neostigmine was used as a positive control. For the compounds which exhibited over 50% inhibition of either AChE or BChE activity, full concentration inhibition curves were produced to evaluate IC_{50} values. All experiments were carried out as triplicate. A non-linear regression analysis of the program PRISM 5.0 (GraphPad, San Diego, California, USA) was used to fit the dose–response curves and to calculate IC_{50} values.

Kinetics study

For determination of mode of inhibition of most potent inhibitor **3f2** against AChE and **3f9** against BChE, changes in the initial velocities of the reaction were measured at different concentrations of inhibitor (0, 0.5, 1.0, and 2.0 µM) using respective substrate concentrations i.e. 0, 0.25, 0.5, 1 and 1.5 mM. A double-reciprocal plot of the inhibition kinetics of AChE by **3f2** and BChE by **3f9** was measured by using PRISM 5.0 (GraphPad, San Diego, California, USA).

Molecular docking

Molecular docking calculations were carried out using FlexX utility of LeadIT from BioSolveIT GmbH, Germany (LeadIT 2011). X-rays structures of equine BChE are currently not available and for electric eel AChE only low crystallographic resolution (>4 Å) structures are available (Saeed et al. 2014). Therefore, X-ray structures of human AChE (PDB ID: 4BDT) and human BChE (PDB ID: 4BDS) were used as template structures and retrieved from RSC Protein Data Bank and used for molecular docking studies (Nachon et al. 2013). Prior to the performance of docking studies the receptor active site was defined as the amino-acid residues in 6.5 Å radius around the co-crystallized ligands. Default parameters of amino acid flips and solvent handling were used. Molecular docking of compounds were then carried out using default docking parameters and 50 top ranking poses were retained for visual inspection in Discovery Studio Visualizer (Studio and Insight 2009) to determine the putative binding mode.

Acknowledgments J. Iqbal is thankful to the Organization for the Prohibition of Chemical Weapons (OPCW), The Hague, The Netherlands and Higher Education Commission of Pakistan for the financial support through Project No. 20-3733/NRPU/R&D/14/520 for the financial support.

Compliance with ethical standards

Conflict of interest The authors declare that they have no competing interests.

References

Aly AA, Ahmed EK, Mokadem KMEl, Hegazy MEAF (2007) Update survey on aroyl substituted thioureas and their applications. J Sulfur Chem 28:73–93

Brouwer MS, Grosscurt AC, Duphar International Research BV (1982) Urea and thiourea compounds and insecticidal compositions. U.S. Patent 4,350,706

Darvesh S, Hopkins DA, Geula C (2003) Neurobiology of butyrylcholinesterase. Nat Rev Neurosci 4:131–138

Dave KR, Syal AR, Katyare SS (2000) Tissue cholinesterases. A comparative study of their kinetic properties. Z Naturforsch C 55:100–108

Ellman GL, Courtney KD, Andres V, Featherstone RM (1961) A new and rapid colorimetric determination of acetylcholinesterase activity. Biochem Pharmacol 7:88–95

Eweis M, Elkholy S, Elsabee M (2006) Antifungal efficacy of chitosan and its thiourea derivatives upon the growth of some sugar-beet pathogens. Int J Biol Macromol 38:1–8

Fukui K (1982) Chemical reactivity theory-its pragmatism and beyond. Pure Appl Chem 54:1825–1836

Gaussian 09, Revision D.01, Frisch MJ, Trucks GW, Schlegel HB, Scuseria GE, Robb MA, Cheeseman JR, Scalmani G, Barone V, Mennucci B, Petersson GA et al. (2009) Gaussian. Inc., Wallingford CT

Gökce H, Bahçeli S (2013) FT-IR, Micro-Raman and UV–Vis spectroscopic and quantum chemical investigations of free 2, 2′-dithiodipyridine and its metal (Co, Cu, and Zn) halide complexes. Spectrochim Acta Mol Biomol Spectrosc 114:61–73

Gopi D, Bhuvaneswaran N, Rajeswarai S, Ramadas K (2000) Synergistic effect of thiourea derivatives and non-ionic surfactants on the inhibition of corrosion of carbon steel in acid environments. Anti-Corrosion Method Mater 47:332–339

Hardy J, Selkoe DJ (2002) The amyloid hypothesis of Alzheimer's disease: progress and problems on the road to therapeutics. Science 297:353–356

Ke SY, Xue SJ (2006) Synthesis and herbicidal activity of *N*-(o-fluorophenoxyacetyl) thioureas derivatives and related fused heterocyclic compounds. Arkivoc 10:63–68

Koch KR (2001) New chemistry with old ligands: *N*-alkyl-and *N*, *N*-dialkyl-N′-acyl (aroyl) thioureas in co-ordination, analytical and process chemistry of the platinum group metals. Coord Chem Rev 216:473–488

Koelle GB (1994) Pharmacology of organophosphates. J Appl Toxicol 14:105–109

Krieter PA, Ziegler DM, Hill KE, Burk RF (1984) Increased biliary GSSG efflux from rat livers perfused wth thiocarbamide substrates for the flavin-containing monooxygenase. Mol Pharmacol 26:122–127

Larik FA, Saeed A, Channar PA, Ismail H, Dilshad E, Mirza B (2016) New 1-octanoyl-3-aryl thiourea derivatives: solvent-free synthesis, characterization and multi-target biological activities. Bangladesh J Pharmacol 11:894–902

LeadIT B (2011) http://www. biosolveit. de/LeadIT. Accessed 12th Mar
Marrs TC, Maynard R (2013) Neurotranmission systems as targets for toxicants: a review. Cell Biol Toxicol 29:381–396
Mertschenk B, Beck F, Bauer W (2002) Thiourea and thiourea derivatives. Ullmann's encyclopedia of industrial chemistry. Wiley-VCH Verlag GmbH & Co. KGaA, Berlin
Nachon F, Carletti E, Ronco C, Trovaslet M, Nicolet Y, Jean L, Renard PY (2013) Crystal structures of human cholinesterases in complex with huprine W and tacrine: elements of specificity for anti-Alzheimer's drugs targeting acetyl-and butyryl-cholinesterase. Biochem J 453:393–399
Nencki M (1873) Zur kenntniss des sulfoharnstoffs. Eur J Inorg Chem 6:598–600
Ren J, Diprose J, Warren J, Esnouf RM, Bird LE, Ikemizu S, Slater M, Milton J, Balzarini J, Stuart DI (2000) Phenylethylthiazolylthiourea (PETT) non-nucleoside inhibitors of HIV-1 and HIV-2 reverse transcriptases structural and biochemical analyses. J Biol Chem 275:5633–5639
Saeed A, Flörke U, Erben MF (2014) A review on the chemistry, coordination, structure and biological properties of 1-(acyl/aroyl)-3-(substituted) thioureas. J Sulfur Chem 35:318–355
Saeed A, Khera RA, Abbas N, Latif M, Sajid I, Floerke U (2010) Synthesis, characterization, crystal structures, and antibacterial activity of some new 1-(3, 4, 5-trimethoxybenzoyl)-3-aryl thioureasreas. Turk J Chem 34:335–346
Saeed A, Mahesar PA, Zaib S, Khan MS, Matin A, Shahid M, Iqbal J (2014) Synthesis, cytotoxicity and molecular modelling studies of new phenylcinnamide derivatives as potent inhibitors of cholinesterases. Eur J Med Chem 78:43–53
Saeed A, Shaheen U, Hameed A, Naqvi SH (2009) Synthesis, characterization and antimicrobial activity of some new 1-(fluorobenzoyl)-3-(fluorophenyl) thioureas. J Fluor Chem 130 (11):1028–1034
Schroeder DC (1955) Thioureas. Chem Rev 55:181–228
Sheldrick GM (2008) A short history of SHELX. Acta Cryst A 64:112–122
Shen Y, Zhang J, Sheng R, Dong X, He Q, Yang B, Hu Y (2009) Synthesis and biological evaluation of novel flavonoid derivatives as dual binding acetylcholinesterase inhibitors. J Enzyme Inhib Med Chem 24:372–380
Smith DA (2009) Treatment of Alzheimer's disease in the long-term-care setting. AJHP 66(10):899–907
Sriram D, Yogeeswari P, Dinakaran M, Thirumurugan R (2007) Antimycobacterial activity of novel 1-(5-cyclobutyl-1, 3-oxazol-2-yl)-3-(sub) phenyl/pyridylthiourea compounds endowed with high activity toward multidrug-resistant *Mycobacterium tuberculosis*. J Antimicrob Chemother 59:1194–1196
Studio D, Insight I (2009) Accelrys Software Inc. San Diego, CA, 92121.
Terry AV, Buccafusco JJ (2003) The cholinergic hypothesis of age and Alzheimer's disease-related cognitive deficits: recent challenges and their implications for novel drug development. J Pharm Exp Ther 306:821–827
Tougu V (2001) Acetylcholinesterase: mechanism of catalysis and inhibition. Curr Med Chem Cent Nerv Syst Agents 1:155–170
Ziegler DM (1978) Intermediate metabolites of thiocarbamides, thioureylenes and thioamides; mechanism of formation and reactivity. Biochem Soc Trans 6:94–96
Ziegler-Skylakakis K, Nill S, Pan JF, Andrae U (1998) *S*-Oxygenation of thiourea results in the formation of genotoxic products. Environ Mol Mutagen 31:362–373